

First-principles study of the blue bronze $K_{0.3}MoO_3$

José-Luis Mozos, Pablo Ordejón, and Enric Canadell

Institut de Ciència de Materials de Barcelona, CSIC, Campus de la U.A.B., 08193 Bellaterra, Barcelona, Spain

(Received 12 March 2002; published 10 June 2002)

The electronic structure of the low-dimensional metal $K_{0.3}MoO_3$ has been studied by means of first-principles density functional calculations. The dispersion of the partially filled bands is found to be in good agreement with the presently available photoemission results. The Fermi surface of this material is shown to be composed of two pairs of slightly warped sheets perpendicular to the highly conducting direction (the b axis) which are nested by the $0.75 b^*$ wave vector. The nature of the relevant states for the conductivity and the electronic instability is discussed. The present results provide a more realistic description of the electronic structure of the blue bronze than the previous tight-binding ones.

DOI: 10.1103/PhysRevB.65.233105

PACS number(s): 71.20.-b, 71.18.+y

Low-dimensional molybdenum and tungsten oxides and bronzes have been the focus of much attention because of the charge density wave (CDW) instabilities they exhibit.¹⁻¹⁰ The discovery of nonlinear transport due to sliding of CDW in the $K_{0.3}MoO_3$ blue bronze⁸ was at the origin of the renewed interest in many of these materials. Even if they are the more intensely studied among them, the blue bronzes still present the low-dimensional community with many puzzling and very fundamental problems: the question of the spin-charge separation, the temperature dependence of the modulation vector, etc.

The understanding of the structural and electronic origin of these CDW instabilities has relied on the availability of calculated band structures and Fermi surfaces.⁷ In some cases the Fermi surface clearly exhibits nesting features which are at the origin of the instabilities. In most cases however, the Fermi surfaces are apparently non-nested and for some time it was difficult to understand the origin of the instabilities. The development of the so-called hidden nesting concept^{5,11} provided a simple way for analyzing the apparently non-nested Fermi surfaces in terms of a superposition of nested ones. These solids have complex unit cells and thus it was only possible to calculate the Fermi surface using extended Hückel-type calculations.⁷ These calculations were remarkably successful and in some cases were predictive. Recent photoemission studies have provided a confirmation for these calculated Fermi surfaces.¹²⁻¹⁸ The agreement was found to be less good for the band dispersion which, when calculated with the extended Hückel method, were found to be too small by at least a factor of 2. In some cases like the blue bronzes there were some noticeable disagreements in the relative dispersion of some bands.

First-principles calculations of the band structure and Fermi surface of this type of materials have only been scarcely reported so far. Yet, in view of recent progress in photoemission studies of these materials, these calculations would be very helpful in rationalizing the experimental data and providing a link between the crystal and electronic structure of these low-dimensional solids. To the best of our knowledge, only the lowest members of the monophosphate tungsten bronzes have been the subject of detailed reports concerning this type of calculations.¹⁹ Here we report a first-principles study of the electronic structure of the potassium

blue bronze, $K_{0.3}MoO_3$, one of the more widely studied CDW materials. $K_{0.3}MoO_3$ is a quasi-one-dimensional (quasi-1D) metal²⁰ which at 180 K undergoes a metal-to-semiconductor transition.²¹ X-ray diffuse scattering studies showed that such transition is associated with an incommensurate CDW instability.²² The basic band structure for this system was reported at the extended Hückel level by Whangbo and Schneemeyer²³ and a more in-depth analysis of the nature of the electronic structure was later reported by Canadell and Whangbo.⁷ Let us note that Kaxiras *et al.*²⁴ have also independently performed a first-principles study of this system although the computational approach employed is different.

The calculations were carried out using a numerical atomic orbitals density functional theory (DFT)^{25,26} approach, which has been recently developed and designed for efficient calculations in large systems and implemented in the SIESTA code.^{27,28} We have used the generalized gradient approximation to DFT and, in particular, the functional of Perdew, Burke, and Ernzerhof.²⁹ Only the valence electrons are considered in the calculation, with the core being replaced by norm-conserving scalar relativistic pseudopotentials³⁰ factorized in the Kleinman-Bylander form.³¹ Nonlinear partial-core corrections to describe the exchange and correlations in the core region were included for Mo.³² We have used a split-valence double- ζ basis set including polarization orbitals for all atoms, as obtained with an energy shift of 500 meV.²⁸ The integrals of the self-consistent terms of the Kohn-Sham Hamiltonian are obtained with the help of a regular real space grid in which the electron density is projected. The grid spacing is determined by the maximum kinetic energy of the plane waves that can be represented in that grid. In the present work, we used a cutoff of 200 Ry, which yields to a spacing between the grid points of around 0.1 Å. The Brillouin zone (BZ) was sampled using a grid of $(5 \times 5 \times 5)$ k points.³³ We have checked that the results are well converged with respect to the real space grid and the BZ sampling.

The crystal structure of $K_{0.3}MoO_3$ is centered monoclinic^{34,35} and contains MoO_3 layers in between which the K atoms reside [see Fig. 1(a)]. The repeat unit of these layers is the $Mo_{10}O_{30}$ group highlighted in Fig. 1(b). The ten octahedral units make chains along the b direction, which is

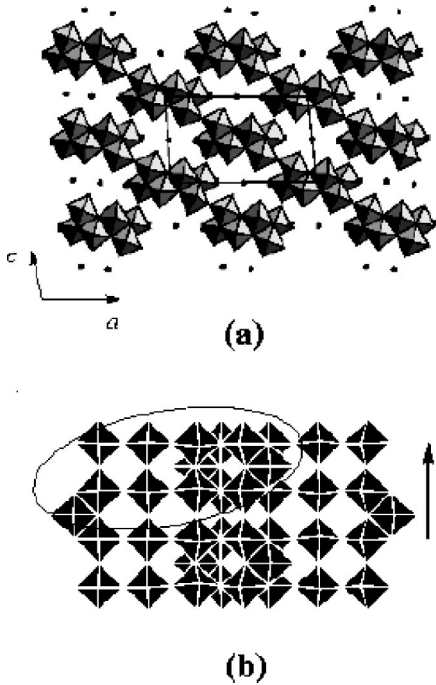


FIG. 1. (a) Projection along the b axis of the crystal structure of $K_{0.3}MoO_3$. The simple monoclinic cell is shown. (b) View of one MoO_3 layer where the basic unit of ten octahedra is highlighted.

also the direction of high conductivity, through both edge and corner-sharing between successive units. Edge-sharing between different chains leads to the MoO_3 layers. As can be easily seen in Fig. 1(b), the chains contain two clearly different types of octahedra: (i) those making quadruple chains of corner-sharing octahedra along b and, (ii) the so-called hump octahedra, sharing two edges with octahedra of the outer part of the quadruple chain. Both bond-strength/bond-length correlations³⁵ and extended Hückel calculations^{7,23} have suggested that the hump octahedra do not really contribute to the conductivity of the blue bronze. Although the chemical formula for the repeat unit of the simple monoclinic cell [shown as a parallelogram in Fig. 1(a)] is $K_6Mo_{20}O_{60}$, the centered nature of the crystal structure allowed us to use a repeat unit half in size. As repeat vectors of the centered lattice we found it convenient to employ $a' = 1/2(-a + b + c)$, $b' = b$ and $c' = c$, where a ($=6.2311$ Å), b ($=7.5502$ Å), and c ($=9.8614$ Å) are the repeat vectors of the simple monoclinic lattice.

The calculated band structure near the Fermi level is shown in Fig. 2(a), and the density of states for a much wider energy range in Fig. 2(b). The density of states diagram exhibits a strong mixing between the molybdenum and oxygen states, clearly showing the covalent character of the binding in the MoO_3 layers. In contrast, the potassium levels practically do not contribute to the filled levels of the system [the potassium contributions are found at energies higher than shown in Fig. 2(b)] confirming that the potassium atoms act as electron donors toward the MoO_3 layers. The bottom of the bands crossing the Fermi level are separated by about 0.35 eV from the top of the valence bands below, which do

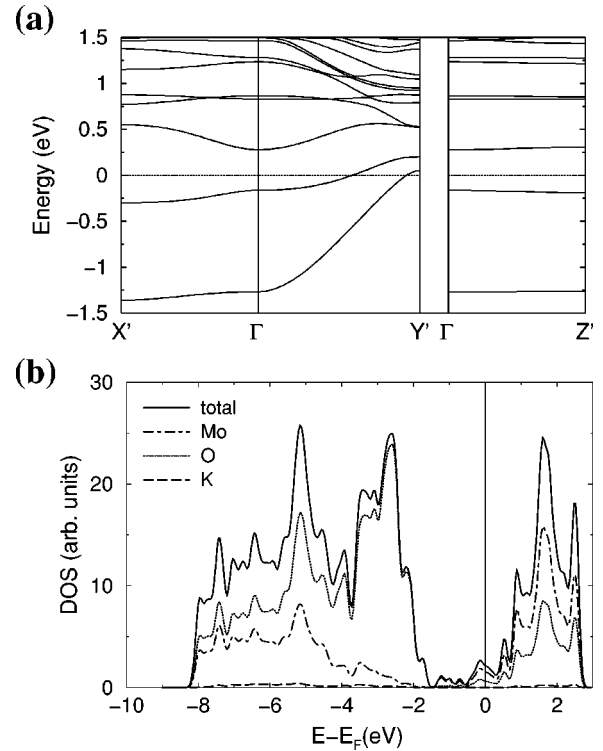


FIG. 2. (a) Band structure near the Fermi level calculated for $K_{0.3}MoO_3$. $\Gamma=(0,0,0)$, $X'=(\frac{1}{2},0,0)$, $Y'=(0,\frac{1}{2},0)$ and $Z'=(0,0,\frac{1}{2})$ in units of the a'^* , b'^* and c'^* reciprocal lattice vectors; (b) Total and projected density of states of $K_{0.3}MoO_3$ projected onto the Mo, O, and K sites.

not contain large contributions of molybdenum and are essentially made of oxygen lone pairs. Although not shown in Fig. 2(b), further decomposition of the molybdenum contribution shows that the levels of molybdenum atoms in the hump octahedra do not contribute to the density of states around the Fermi level, confirming the previous more qualitative results.

As shown in Fig. 2(a), there are two partially filled bands with very strong one-dimensional character. The two bands have noticeably different dispersions along the chain direction, with a considerably larger energy difference at Γ , whereas they run in an almost parallel way in the previous extended Hückel band structure.²³ The lower band is between four and five times more dispersive in the present calculations. These facts are in good agreement with both the photoemission results^{12,14,17,18} and the plane-wave calculations²⁴ so that the previous quantitative disagreement between the experimental and theoretical band structures of the blue bronze seems now to be solved (see Fig. 3). The lower band is cut by the Fermi level at 86% of π/b whereas the upper band is cut at 57% of π/b . Again, these values are in excellent agreement with those given by the most recent photoemission studies, 90% and 59%, respectively.¹⁸

In order to give a more complete description of the nature of the partially filled bands we show in Fig. 4 a representation of the crystal orbitals at Γ for the two partially filled bands. These levels are essentially built from Mo d_{xz} -type orbitals (we assume a set of local coordinate axis in which z

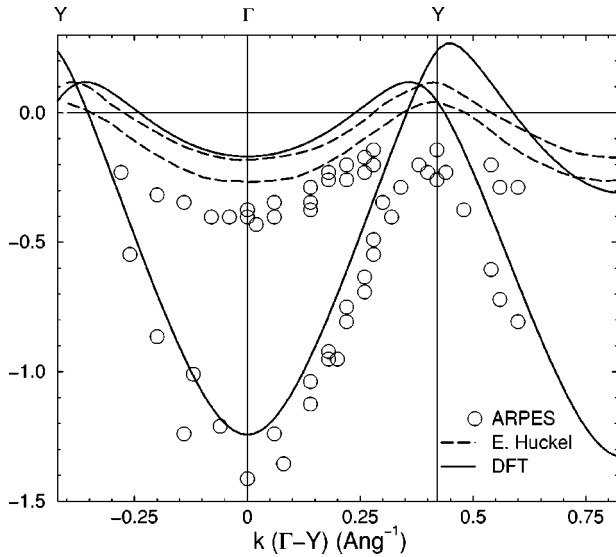


FIG. 3. Comparison of the ARPES (from Ref. 12) and the calculated band structure (previous tight-binding—Ref. 23—and present DFT results) for the blue bronze.

is the direction of the chains and the MoO_3 layers are in the xz plane). In both of these levels the contribution of the d orbitals of the hump octahedra is practically nil. All d_{xz} orbitals are in-phase in the lower band [see Fig. 4(a)] so that the local pseudosymmetry is such that the O p_z and p_x practically cannot mix into it and thus, it is the lowest Mo d -based level at the Γ point. The second band [Fig. 4(b)] has opposite parity with respect to the twofold screw axis. Consequently, the O p_z levels mix in an antibonding way at the center of the quadruple octahedral chain. Because of the normalization condition, the contributions of the Mo d_{xz} orbitals of the inner and outer octahedra of the quadruple chains become more different, breaking the local pseudosymmetry and allowing a smaller but significant antibonding mixing of the other O p_z orbitals. This description is in good agreement with the previous qualitative discussion based on simple tight-binding ideas.⁷ What this description also makes clear is that the reason for the difference between the first-principles calculations and the previous extended Hückel results is that the Mo d_{xz} -O p_z interactions are considerably underestimated in the latter. The enhanced antibonding mix-

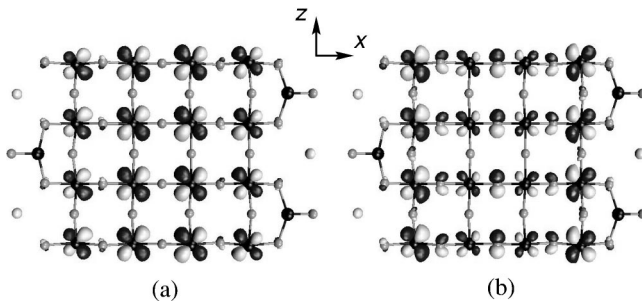


FIG. 4. Nature of wave functions associated with the two partially filled bands of the blue bronze at the Γ point: (a) lower and, (b) upper band. The Mo, O, and K atoms are depicted in black, dark, and light gray colors, respectively.

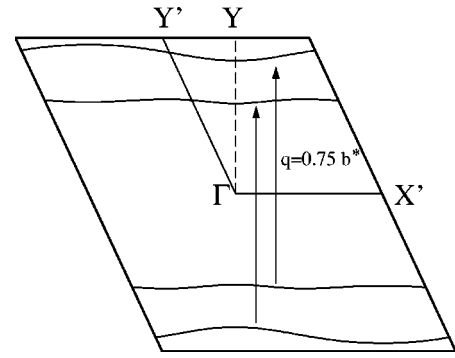


FIG. 5. (a', b') plane of the Fermi surface calculated for $\text{K}_{0.3}\text{MoO}_3$. $\Gamma=(0,0,0)$, $X'=(a'/2,0,0)$, $Y'=(0,b'/2,0)$ and $Y=(0,b'/2,0)$. The q nesting vector is indicated.

ing of O p_z and the increased differentiation between the Mo d_{xz} contributions of the inner and outer octahedra of the quadruple chains via the normalization condition, make the energy difference between the two bands at the Γ and Y' points very different.

The band dispersion along the interlayer direction is extremely small so that in Fig. 5 we just report the calculated Fermi surface in the (a', b') plane of the Brillouin zone. It contains two pairs of slightly warped lines perpendicular to the chain direction. The warping is clearly smaller than in the previous tight binding calculations, something which was already suggested by photoemission studies.¹² In fact, the energy associated with the warping of both lines is such that it is practically irrelevant at the temperature of the metal-to-semiconductor transition. Thus, a single nesting vector can lead to the destruction of the complete Fermi surface without the need to invoke opposite curvatures of the two partially filled bands along the direction perpendicular to the chains.^{23,36} The calculated nesting vector ($q=0.75b^*$) is in fact imposed by the electron conservation rule once the effectively one-dimensional nature of the Fermi surface is accepted. Thus, the question of why the CDW wave vector is incommensurate ($q=0.72b^*$) at 180 K immediately arises. Another interesting result of the present study is the absence of any empty band lying very near the Fermi level that could be populated by thermal activation. The existence of such a low-lying band was proposed³⁶ in order to provide a rationale for the variation of the CDW wave vector with temperature as well as the contrasting behavior of resistivity and susceptibility in the normal metallic state (i.e., the resistivity is typical of a metallic system while the susceptibility exhibits a gapped behavior). This low-lying band does indeed exist in the previous extended Hückel band structure but no evidence has been found in the photoemission studies. This band is also not found in the independent first-principles study by Kaxiras *et al.*²⁴ The reason for the discrepancy between the extended Hückel and the first-principles calculations lies in the above-mentioned underestimation of the Mo d_{xz} -O p_z antibonding interactions which leaves the third band at Γ [see Figure 2(a)] too low in energy. Anyway, this result is significant in that it suggests that alternative explanations for the temperature dependence of the CDW wave

vector and the apparent spin-charge separation in the normal state must be looked for. Those provided for instance by Voit (temperature dependence of the susceptibility)³⁷ or by Noguera and Pouget³⁸ (temperature dependence of the wave vector) certainly deserve further attention.

In summary, the present first-principles calculations provide a description of the electronic structure of the $K_{0.3}MoO_3$ blue bronze in clearly better quantitative agreement with the more recent photoemission studies than the previous tight-binding ones. Thus, it is hoped that they provide a firmer

ground upon which to discuss the new experiments designed to clarify the still puzzling features of the electronic structure of this low-dimensional material.

This work was supported by the DGI-Spain (Project No. BFM2000-1312-C02-01), Generalitat de Catalunya (2001SGR 00333) and by grants of computer time from the CESA-CEPBA. We thank Professor R. Claessen for informing us of the independent theoretical study by Kaxiras and co-workers.

-
- ¹*Low-Dimensional Electronic Properties of Molybdenum Bronzes and Oxides*, edited by C. Schlenker (Kluwer, Dordrecht, 1989).
- ²*Physics and Chemistry of Low-Dimensional Inorganic Conductors*, edited by C. Schenker, J. Dumas, M. Greenblatt, and S. van Smaalen, NATO ASI Series B, Physics Vol. 354 (Plenum, New York, 1996).
- ³M. Greenblatt, *Int. J. Mod. Phys. B* **7**, 3937 (1993).
- ⁴P. Foury and J.-P. Pouget, *Int. J. Mod. Phys. B* **7**, 3973 (1993).
- ⁵E. Canadell and M.-H. Whangbo, *Int. J. Mod. Phys. B* **7**, 4005 (1993).
- ⁶J. Dumas and C. Schlenker, *Int. J. Mod. Phys. B* **7**, 4045 (1993).
- ⁷E. Canadell and M.-H. Whangbo, *Chem. Rev.* **91**, 965 (1991).
- ⁸J. Dumas, C. Schlenker, J. Marcus, and R. Buder, *Phys. Rev. Lett.* **50**, 757 (1983).
- ⁹E. Wang, M. Greenblatt, I.E.-I. Rachidi, E. Canadell, M.-H. Whangbo, and S. Vadlamannati, *Phys. Rev. B* **39**, 12 969 (1989).
- ¹⁰J. Dumas, C. Hess, C. Schlenker, G. Bonfait, E. Gomez Marin, D. Groult, and J. Marcus, *Eur. Phys. J. B* **14**, 73 (2000).
- ¹¹M.-H. Whangbo, E. Canadell, P. Foury, and J.-P. Pouget, *Science* **252**, 96 (1991).
- ¹²G.-H. Gweon, J.W. Allen, R. Claessen, J.A. Clack, D.M. Poirier, P.J. Benning, C.G. Olson, W.P. Ellis, Y.X. Zhang, L.F. Schneemeyer, J. Marcus, and C. Schlenker, *J. Phys.: Condens. Matter* **8**, 9923 (1996).
- ¹³K.E. Smith, K. Breuer, M. Greenblatt, and W. McCarroll, *Phys. Rev. Lett.* **70**, 3772 (1993).
- ¹⁴M. Grioni, H. Berger, M. Garnier, F. Bommeli, L. Degiorgi, and C. Schlenker, *Phys. Scr.*, **T66**, 172 (1996); L. Perfetti, S. Mitrovic, G. Margaritondo, M. Grioni, R. Gaál, L. Forró, L. Degiorgi, and H. Höchst, *Phys. Rev. B* (submitted).
- ¹⁵K. Breuer, C. Stagaescu, K.E. Smith, M. Greenblatt, and K. Ramanujachary, *Phys. Rev. Lett.* **76**, 3172 (1996).
- ¹⁶M. Grioni and J. Voit, in *Electron Spectroscopies Applied to Low-dimensional Materials*, edited by H. Stanberg and H. P. Hughes (Kluwer, Dordrecht, 2000), p. 209.
- ¹⁷A.V. Fedorov, S.A. Brazovskii, V.N. Muthukumar, P.D. Johnson, J. Xue, L.C. Duda, K.E. Smith, W.H. MacCarroll, M. Greenblatt, and S.L. Hulbert, *J. Phys.: Condens. Matter* **12**, L191 (2000).
- ¹⁸G.H. Gweon, J.D. Denlinger, J.W. Allen, R. Claessen, C.G. Olson, H. Höchst, J. Marcus, C. Schlenker, and L.F. Schneemeyer, *J. Electron Spectrosc. Relat. Phenom.* **117-118**, 481 (2001).
- ¹⁹E. Sandré, P. Foury-Leylekian, S. Ravy, and J.-P. Pouget, *Phys. Rev. Lett.* **86**, 5100 (2001); P. Foury-Leylekian, E. Sandré, S. Ravy, J. -P. Pouget, E. Elkaim, P. Roussel, D. Groult, and Ph. Labbé, *Phys. Rev. B* (submitted).
- ²⁰G. Travaglini, P. Wachter, J. Marcus, and C. Schlenker, *Solid State Commun.* **37**, 599 (1971).
- ²¹C. Schlenker and J. Dumas, in *Crystal Chemistry and Properties of Materials with Quasi-One-Dimensional Structures*, edited by J. Rouxel (Reidel, Dordrecht, 1986), p. 135.
- ²²J.-P. Pouget, S. Kagoshima, C. Schlenker, and J. Marcus, *J. Phys. (France) Lett.* **44**, L113 (1983).
- ²³M.-H. Whangbo and L.F. Schneemeyer, *Inorg. Chem.* **25**, 2424 (1986).
- ²⁴The results have been partially published in: U.V. Waghmare, H. Kim, I.J. Park, N. Modine, P. Maragakis, and E. Kaxiras, *Comput. Phys. Commun.* **137**, 341 (2001).
- ²⁵P. Hohenberg and W. Kohn, *Phys. Rev.* **136**, 864 (1964).
- ²⁶W. Kohn and L.J. Sham, *Phys. Rev.* **140**, 1133 (1965).
- ²⁷D. Sánchez-Portal, P. Ordejón, E. Artacho, and J.M. Soler, *Int. J. Quantum Chem.* **65**, 453 (1997).
- ²⁸E. Artacho, D. Sánchez-Portal, P. Ordejón, A. García, and J.M. Soler, *Phys. Status Solidi B* **215**, 809 (1999).
- ²⁹J.P. Perdew, K. Burke, and M. Ernzerhof, *Phys. Rev. Lett.* **77**, 3865 (1996).
- ³⁰N. Trouiller and J.L. Martins, *Phys. Rev. B* **43**, 1993 (1991).
- ³¹L. Kleinman and D.M. Bylander, *Phys. Rev. Lett.* **48**, 1425 (1982).
- ³²S.G. Louie, S. Froyen, and M.L. Cohen, *Phys. Rev. B* **26**, 1738 (1982).
- ³³H.J. Monkhorst and J.D. Park, *Phys. Rev. B* **13**, 5188 (1976).
- ³⁴J. Graham and A.D. Wadsley, *Acta Crystallogr.* **20**, 93 (1966).
- ³⁵M. Ghedira, J. Chenavas, M. Marezio, and J. Marcus, *J. Solid State Chem.* **57**, 300 (1985).
- ³⁶J.-P. Pouget, C. Noguera, A. Moudden, and R. Moret, *J. Phys. (France)* **46**, 1731 (1985).
- ³⁷J. Voit, *Eur. Phys. J. B* **5**, 505 (1998).
- ³⁸C. Noguera and J.-P. Pouget, *J. Phys. I* **1**, 1053 (1991).